Electronic Supplementary Information

Strength of Attraction: Pyrene-Based Hole-Transport Materials with Effective π-π Stacking for Dopant-free Perovskite Solar Cells

Marina Tepliakova,*[a] Igor K. Yakushenko,[b] Elena I. Romadina,[a,b] Artyom V. Novikov,[a,b] Petr M. Kuznetsov,[b] Keith J. Stevenson,[a] and Pavel A. Troshin[a,b]

[a]Skolkovo Institute of Science and Technology, Nobel st. 3, 143026 Moscow, Russia

[b]Institute for Problems of Chemical Physics of Russian Academy of Sciences (IPCP RAS), Semenov av. 1, 142432, Chernogolovka, Moscow region, Russia

Materials

Solvents and reagents were purchased from Sigma-Aldrich or Acros Organics and used as received or purified according to standard procedures, if else is not stated.

The organic materials applied in this work were synthesized according to the previously reported procedures: PCBA (Hummelen *et. al*. J. Org. Chem., **1995**, 60, 532.), PTAA (M. M. Tepliakova *et. al.*, Tetrahedron Lett, **2020**, DOI: 10.1016/j.tetlet.2020.152317152317), pyrene derivatives **Y1**-**Y4** (Kaplunov *et. al.*, Mendeleev Commun., **2016**, 26, 437; I. K. Yakushenko, RU Patent 2572414, issued 10.01.2016).

Device fabrication and characterization

Devices were fabricated as described previously (Tsarev *et. al.* J. Phys. Chem. C, **2020**, 124, 1872–1877). Glass/ITO substrates (Kintec, 15 Ω/sq.) were sequentially cleaned with acetone, distilled water and isopropanol and with air plasma for 5 min. The SnO_2 (Alfa Aesar, 15% aqueous solution) was 1.5 times diluted and spin-coated at 4000 rpm. The samples were heated for 30 min in air at 175°C and then transferred to the glovebox. The samples were heated for 10 min in the inert atmosphere at 150°C, cooled to the room temperature and coated with PCBA (0.5 mg/ml in chlorobenzene). The perovskite ink based on 1.4M solution of PbI_2 and CH_3NH_3I precursors in the mixture of DMF:NMP (4:1) was prepared. Perovskite ink (70 µL) was spin-coated atop the PCBA layer at 4000 rpm and quenched with toluene (160 µL) after 20 s of rotation. The perovskite films were heated for 5 minutes at 80°C inside the glove box. The HTL materials (**Y1, Y2, Y3, Y4** and PTAA as a reference) were spin-coated from chlorobenzene solution (concentrations 10,7,7, 4 and 6 mg mL^{-1} respectively) or thermally evaporated (only for pyrene derivatives) under reduced pressure (10^{-5} mbar). Molybdenum (VI) oxide (10 nm) and silver electrodes (100 nm) were evaporated through shadow mask defining the active area of the electrodes as 0.08 cm^2.

The current-voltage characteristics of the devices were measured under nitrogen atmosphere using the Advantest 6240A source-measurement units and simulated AM1.5 G illumination (100 mW cm^{-2}) provided by Newport Verasol AAA class solar simulator.

The thickness of the evaporated pyrene layers was additionally measured using scratch profiling with atomic NTEGRA PRIMA (NT-MDT, Russia) force microscope.

The charge carries mobility measurements were performed using SCLC method according to the previously reported procedure (Kuznetsov *et. al.* Tetrahedron Lett., 2020, 61, 26). The measurements were carried out in the hole-only devices with configuration ITO/PEDOT:PSS/**Y1-Y4**/VO_x/Ag. The used glass/ITO substrates (Kintec, 15 Ω/sq.) were sequentially cleaned with acetone, distilled water and isopropanol and with air plasma for 5 min. The PEDOT:PSS solution (Clevios PH1000) was diluted with an equal volume of deionized water and spin-coated in the air at 2000 rpm. The samples were annealed for 20 min in air at 165°C and then transferred to the glovebox. The HTL materials (**Y1, Y2, Y3, Y4**) were thermally evaporated under reduced pressure (10^{-5} mbar) to produce a series of samples with thickness ranging from 50 to 400 nm. Vanadium (V) oxide (25 nm) was evaporated on the full area, and silver electrodes (100 nm) were evaporated through a shadow mask. The dependence of the SCLC hole mobility from the thickness of the semiconductor layer was analyzed to account for interface-induced effects occurring typically in the case of relatively thin films (thickness below 100 nm).

The cyclic voltammetry measurements were performed according to the previously reported procedure (Akkuratov *et. al.,* Tetrahedron Lett., 2017, 58, 1, 97-100). The pyrene films were deposited on a glassy carbon disc electrode (working electrode, d = 5 mm, BASInc.) by drop-casting from chlorobenzene. The measurements were performed in a three-electrode electrochemical cell using 0.1 M solution of tetra-n-butylammonium tetrafluoroborate in acetonytrile as a supporting electrolyte, platinum wire as a counter electrode, and $Ag/AgNO_3$ reference electrode (BAS Inc.). Ferrocene was used as an internal reference. The electrolyte solution was purged with argon before the measurements. The voltammograms were recorded using a Metrohm Autolab potentiostat at room temperature with a potential sweep rate of 200 mV s^{-1}.

The water contact angle on the evaporated films of **Y1**-**Y4** (50 nm) was measured using a Kruss Drop Shape Analyzer.

Thermal stability was investigated using TGA-2 thermogravimetric analyzer (Mettler Toledo) at a heating rate of 10°C min^{-1} in inert nitrogen atmosphere.

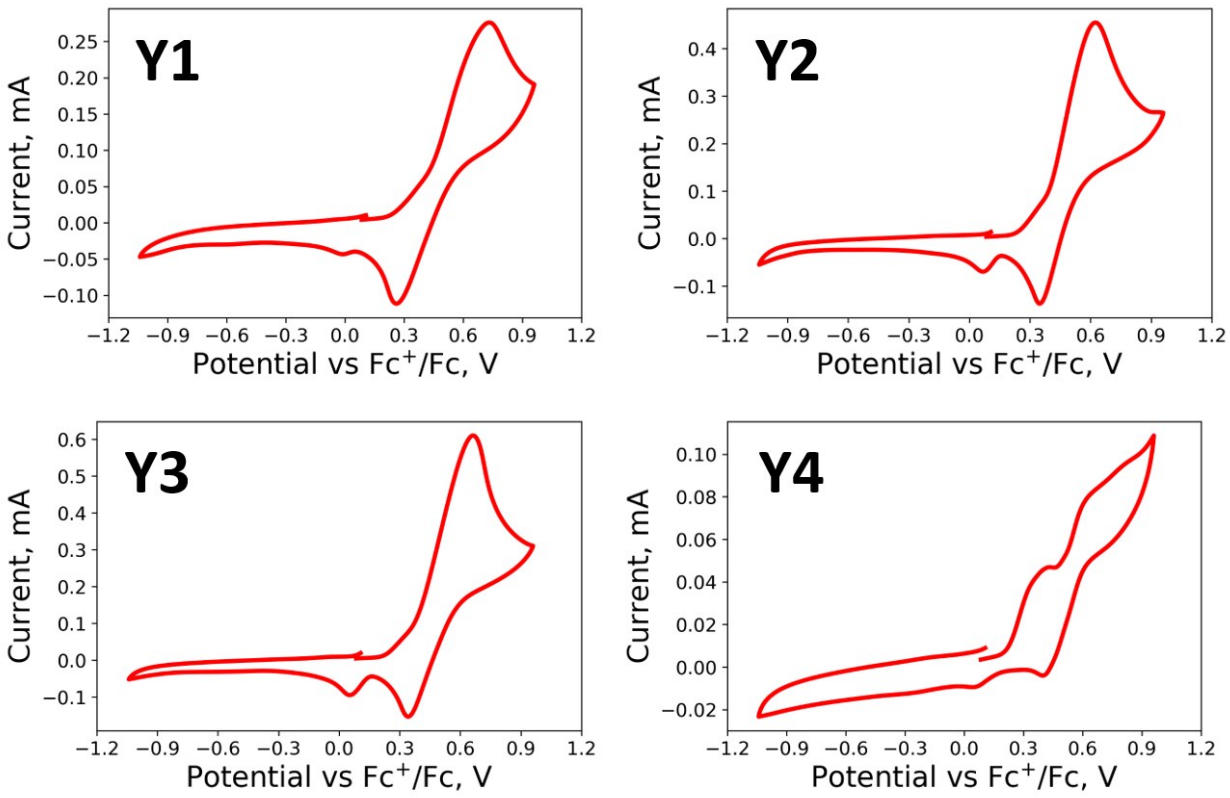

Figure S1. Cyclic voltammograms for thin films of pyrene derivatives **Y1**-**Y4**

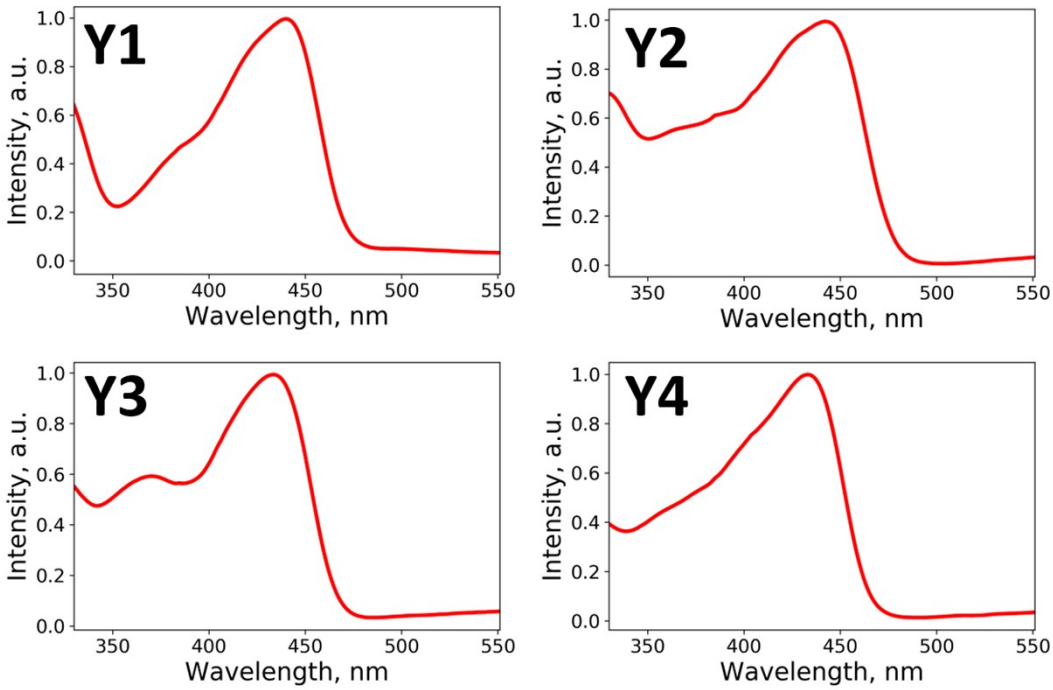

Figure S2. Absorption spectra for thin films of pyrene derivatives **Y1-Y4**

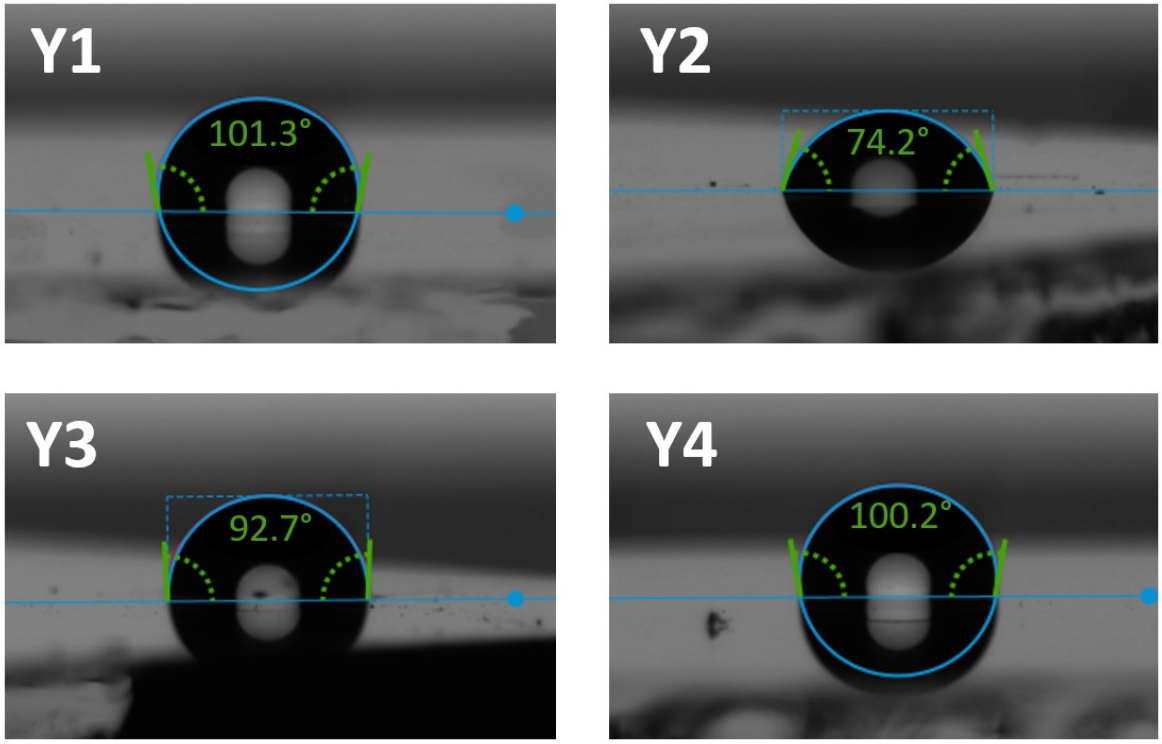

Figure S3. Contact angle measurements for thin films of **Y1-Y4**

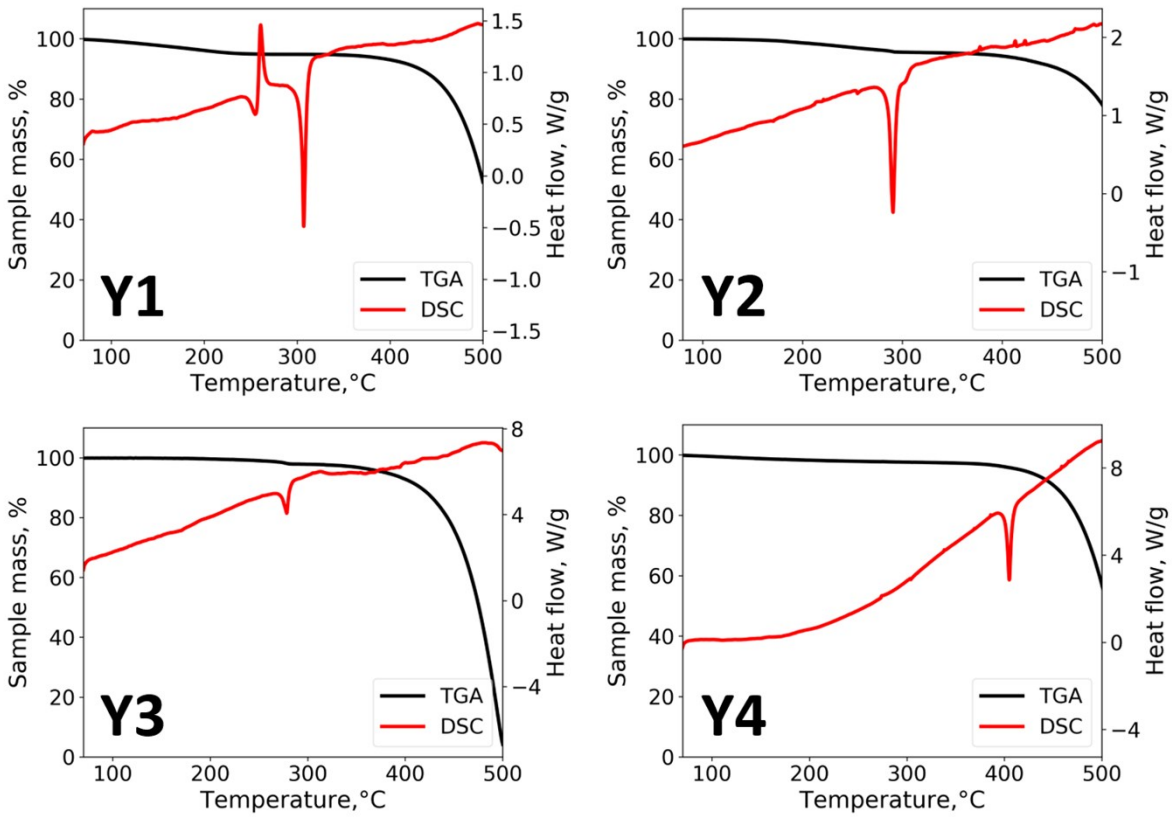

Figure S4. TGA and DSC curved for pyrene derivatives **Y1-Y4**.

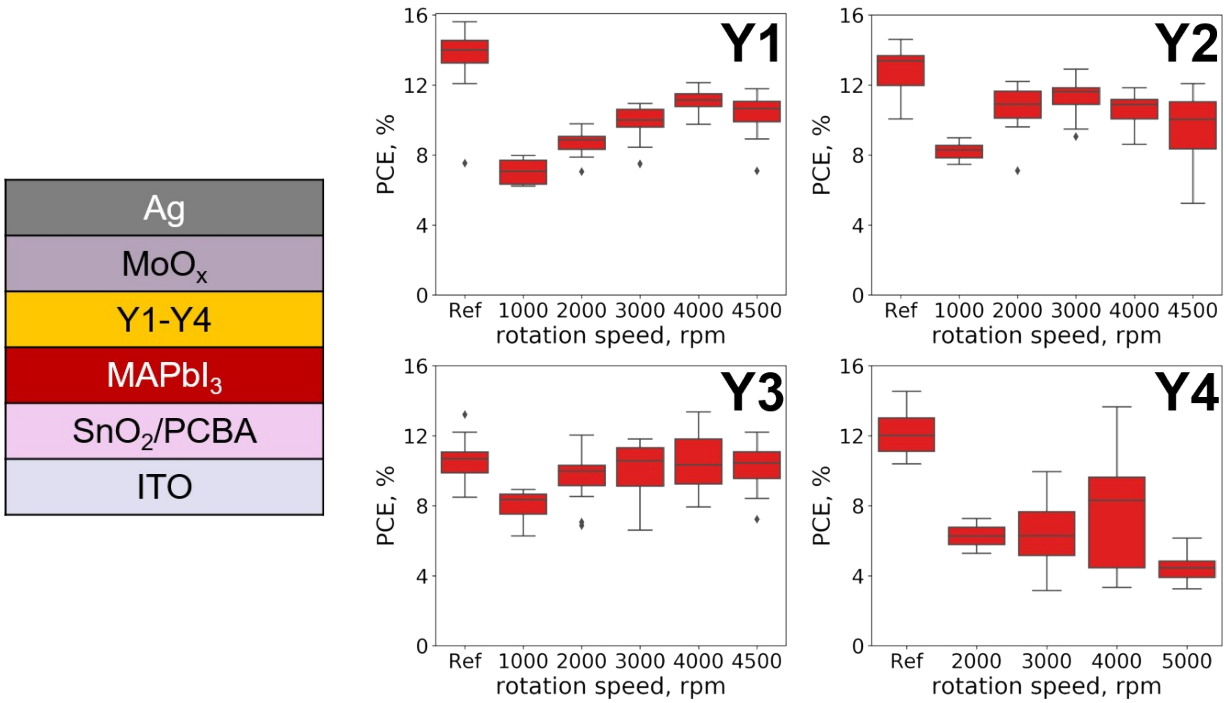

Figure S5. Optimization of the HTL thickness when processing **Y1-Y4** films by spin-coating

Table S1. Characteristics of PSCs assembled with spin-coated **Y1**-**Y4** HTL films

Speed, rpm	V_{oc} , mV		J_{sc} , mA/cm^2		FF, %		PCE, %	
	avg±std	best	avg±std	best	avg±std	best	avg±std	best
Y1 (10 mg mL^{-1} solution in chlorobenzene)								
1000	930±40	966	21.2±0.8	21.8	37±2	39	7.1±0.7	8.0
2000	950±50	986	19.1±0.9	20.0	49±2	52	8.9±0.7	9.8
3000	940±40	980	19.6±0.7	20.1	55±3	58	10.0±0.9	11.0
4000	970±20	994	20.0±1.0	20.2	59±2	65	11.1±0.6	12.1
4500	920±30	967	19.5±0.4	20.0	59±5	63	11.0±1.0	11.8
Ref	1000±30	1019	19.9±0.6	20.1	72±7	77	14.0±2.0	15.6
Y2 (7 mg mL^{-1} solution in chlorobenzene)								
1000	1020±20	1026	18.2±0.4	18.2	44±3	50	8.3±0.4	9.0
2000	1013±9	1019	19.7±0.6	19.9	65±1	65	13.0±0.4	13.2
3000	1000±20	1020	20.2±0.4	20.4	63±1	65	12.5±0.5	13.6
4000	1002±8	1025	19.8±0.2	20.1	66±1	67	13.2±0.2	13.4
4500	980±10	995	20.2±0.1	20.1	64±1	65	12.7±0.2	12.9
Ref*	970±50	1023	19.9±0.3	20.5	58±7	64	11.0±2.0	13.2
Y3 (7 mg mL^{-1} solution in chlorobenzene)								
1000	1030±70	1050	17.6±0.3	17.9	47±3	50	8.4±0.9	8.9
2000	1000±70	1045	18.8±0.6	19.7	54±5	59	10.0±2.0	12.0
3000	990±60	1019	19.3±0.8	19.5	55±6	61	11.0±2.0	11.8
4000	990±60	1047	19.1±0.5	19.6	56±6	66	10.0±2.0	13.4
4500	970±60	1011	19.3±0.7	19.6	56±6	66	11.0±2.0	12.2
Ref	900±30	957	20.0±0.3	20.2	58±6	70	11.0±1.0	13.2
Y4 (4 mg mL^{-1} solution in chlorobenzene)								
2000	720±80	775	18.7±0.1	18.8	46±5	49	6.0±1.0	7.3
3000	900±200	995	16.0±2.0	18.7	50±5	55	6.0±2.0	10.0
4000	900±200	959	19.0±0.9	20.6	51±8	70	8.0±3.0	13.7
5000	700±200	757	18.2±0.7	18.7	36±6	47	4.0±1.0	6.1
Ref	990±10	1004	21.2±0.1	21.4	58±6	68	12.0±2.0	14.5

*Ref stays for reference devices using PTAA as HTL material.

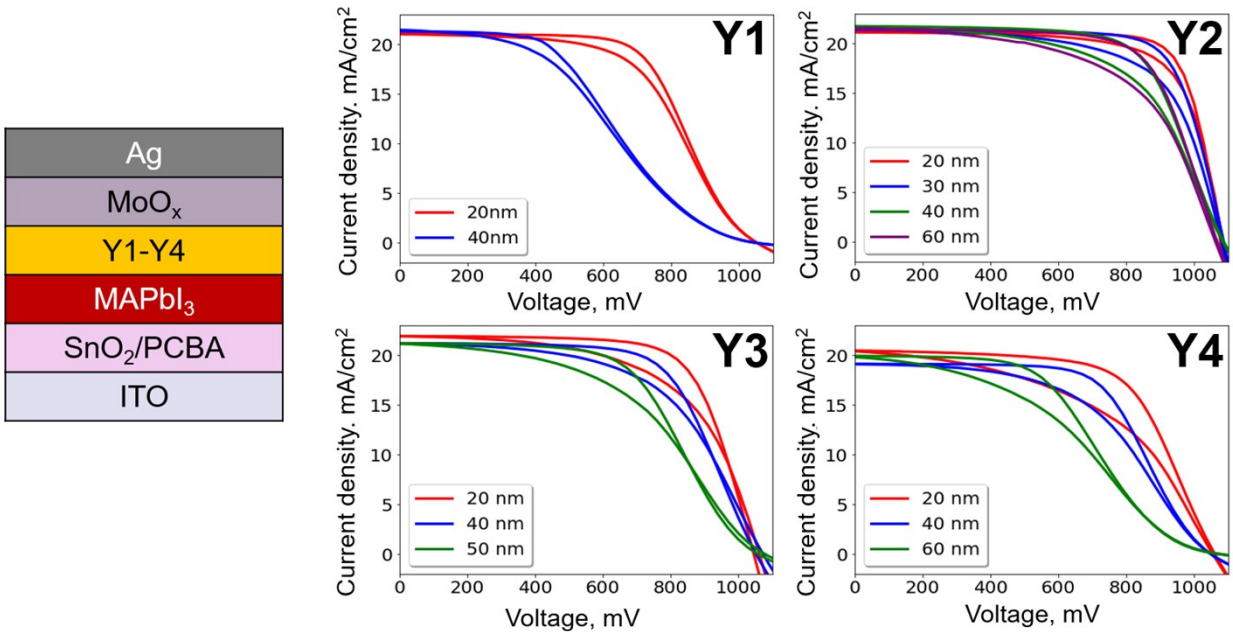

Figure S6. Optimization of the HTL thickness when processing **Y1-Y4** films by thermal evaporation in vacuum

Table S2. Characteristics of PSCs using evaporated **Y1**-**Y4** HTL films

Thickness, nm	V_{oc} , mV		J_{sc} , mA/cm^2		FF, %		PCE, %	
	avg±std	best	avg±std	best	avg±std	best	avg±std	best
Y1								
20	1061±7	1072	21.0±1.0	22.2	55±4	61	12.0±1.0	14.2
40	1050±30	1056	21.2±0.7	21.6	37±2	40	8.3±0.5	9.0
Y2								
20	1090±10	1103	21.1±0.5	21.2	72±5	78	16.0±1.0	17.9
25	1070±10	1099	20.6±0.4	21.3	66±6	75	15.0±2.0	17.1
30	1077±5	1087	20.9±04	21.5	67±5	75	15.0±1.0	17.3
40	1086±7	1092	21.7±0.7	23.2	60±5	67	14.0±1.0	16.1
50	1066±6	1075	20.5±0.1	20.7	61±8	70	13.0±2.0	15.4
60	1070±20	1093	20.8±0.4	21.8	57±7	69	13.0±1.0	15.1
Y3								
20	1050±10	1062	21.0±0.7	22.0	66±5	70	14.0±1.0	16.1
40	1050±10	1082	21.0±0.5	21.2	55±6	64	12.0±1.0	14.5
50	1050±20	1079	20.7±0.6	21.2	48±5	57	10.6±0.9	12.6
Y4								
20	1050±10	1061	21.0±0.3	21.5	55±7	64	12.0±2.0	14.5
30	1060±30	1074	20.6±0.8	21.7	53±7	63	12.0±2.0	13.8
40	1030±80	1082	20.0±1.0	21.8	43±5	53	8.5±0.9	10.3

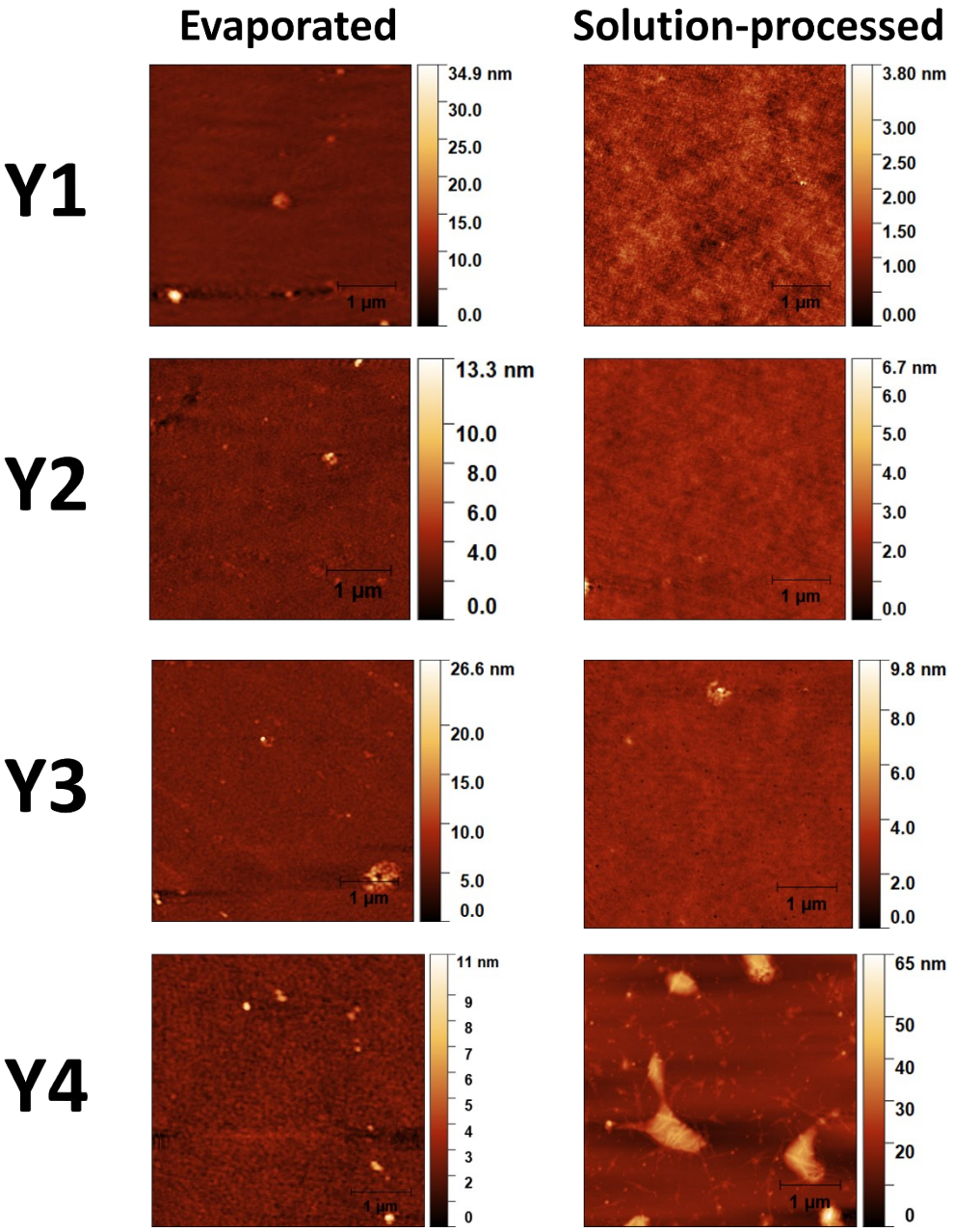

Figure S7. AFM topography images of solution-processed and evaporated films of pyrene derivatives**Y1-Y4**